J. Biomed. Eng. Res.
Vol.26, No.6, 357-363, 2005

Detection of Pulmonary Region in Medical Images through Improved Active Control Model

Yong-Jun Kwon[1], Chul-Ho Won[2], Dong-Hun Kim[1], Pil-Un Kim[3], Il-Yong Park[4], Hee-Jun Park[1], Jyung-Hyun Lee[1], Myoung-Nam Kim[5], Jin-Ho Cho[1,4]

[1]School of Electrical Engineering & Computer Science, Kyungpook National University
[2]Dept. of Computer Control Engineering, Kyungil University
[3]Dept. of Biological & Medical Engineering, Kyungpook National University
[4]Advanced Research Center for Recovery of Human Sensibility, Kyungpook National University
[5] Dept. of Biomedical Engineering, School of Medicine, Kyungpook National University
(Received April 7, 2005. Accepted September 23, 2005)

Abstract: Active contour models have been extensively used to segment, match, and track objects of interest in computer vision and image processing applications, particularly to locate object boundaries. With conventional methods an object boundary can be extracted by controlling the internal energy and external energy based on energy minimization. However, this still leaves a number of problems, such as initialization and poor convergence in concave regions. In particular, a contour is unable to enter a concave region based on the stretching and bending characteristic of the internal energy. Therefore, this study proposes a method that controls the internal energy by moving the local perpendicular bisector point of each control point on the contour, and determines the object boundary by minimizing the energy relative to the external energy. Convergence at a concave region can then be effectively implemented as regards the feature of interest using the internal energy, plus several objects can be detected using a multi-detection method based on the initial contour. The proposed method is compared with other conventional methods through objective validation and subjective consideration. As a result, it is anticipated that the proposed method can be efficiently applied to the detection of the pulmonary parenchyma region in medical images.

Key words: Active contour model, Internal energy, External energy, Control point, Concavity

INTRODUCTION

Extracting the pulmonary parenchyma from a pulmonary image is important for the early detection of a local pulmonary function disorder and diffuse pulmonary disease, a progress monitoring, and medical examinations based on quantitatively measuring the pulmonary parenchyma density and identifying the density distribution curve[1,2]. There are several ways of detecting a closed contour. The first and simple method is based on threshold, where the pulmonary parenchyma is detected by determining a proper threshold and creating a binary image using the histogram distribution. However, setting the proper threshold is difficult and a region with a similar luminance level can be simultaneously detected[3]. The use of an edge operator is also a straightforward method, however, since a closed contour can not be obtained[4], an edge tracing method is also needed to extract the pulmonary parenchyma contour after obtaining the intensity and direction information of the edge using a directional edge operator. Nonetheless, subtle noise can also be detected as a contour[5].

More recently, closed contours are detected using an active contour model considering the shape of the region of interest and image features. An active contour model detects the contour of the object of interest by minimizing the energy controlling the internal and external energy, as originally proposed by Kass et al[6]. However, this method is decisively affected by limited conditions related to the derivative possibility of the energy numerical formula and initialization. To overcome these problems, several methods have already proposed. For example, the application of dynamic programming[7] provides more stability, yet the algorithm is extremely slow, computationally complex, and time consuming. A greedy algorithm[8] can improve the stability,

This study was supported by a grant of the Korea Health 21 R&D Project, Ministry of Health & Welfare, Republic of Korea. (02-PJ3-PG6-EV10-0001)
Corresponding Author : Chul-Ho Won
33 Buho-ri Hayang-up Kyungsan-si Kyungbuk, 712-701, KOREA
Tel. 053-850-7325 Fax. 053-850-7612
H. P. 010-6780-7325
E-mail: chulho@kiu.ac.kr

flexibility, and speed, but non-optimal solution is often produced without using the information obtained in the previous step. Furthermore, conventional active contour models also have a problem with concave regions, as in this case the contour of the object cannot be extracted, since the movement of the contour does not progress in a concave region.

To overcome the concave problem, the new external energy called the Gradient Vector Flow (GVF) is proposed by Xu et al.[9,10] This field is calculated by gradient vector diffusion of binary or gray scale edge map. However, this model is unable to detect several objects.

Accordingly, this paper uses energy minimization to solve the concave problem based on controlling the internal energy moving from each control point assigned in the contour to the local perpendicular bisector. Then, multiple objects can be detected in relation to the initial contour by dividing the contour based on a comparison of a minimal interval for the contour progressing between objects. Previously, a density distribution curve was analyzed by extracting pulmonary parenchyma from pulmonary Electro Beam Computerized Tomography (EBT) images, then several parameters were generated from this analysis for the early diagnosis of diffuse pulmonary diseases and functional disorders of the local pulmonary. Therefore, this paper investigates a variational approach for energy minimization as an initial active contour model, and analyzes the proposed method as a solution to the concave problem and for detecting multiple objects. The effectiveness of the proposed method is then confirmed by applying to pulmonary EBT images.

INITIAL ACTIVE CONTROL MODEL

The original active contour model was introduced as "snakes" and derived by a variational principle from a nongeometric measure. The model starts from an energy function that includes "internal" and "external" terms that are integrated along a contour. Let the contour $v(s) = [x(s), y(s)]$, where $s \in [0,1]$ is an arbitrary parameterization. The active contour model moves through the spatial domain of an image to minimize the energy function. That is, the contour is detected by minimizing the energy function by matching the internal energy and external energy, as in Eq. (1).

$$E_{snake} = \int_0^1 E_{snake}(v(s))ds$$
$$= \int_0^1 (E_{int}(v(s)) + E_{ext}(v(s)))ds \quad (1)$$

where, E_{int} denotes the internal energy of the active contour and E_{ext} is derived from the input image as the external energy. E_{int} depends on the intrinsic character of the curve as a summation of the elastic energy and bending energy to discourage stretching and bending, as in Eq. (2).

$$E_{int} = E_{elastic} + E_{bending}$$
$$= \int_0^1 \frac{1}{2}(\alpha|v_s(s)|^2 + \beta|v_{ss}(s)|^2)ds \quad (2)$$

where α and β are the weighting parameters that control the tension and rigidity of the active contour model, respectively, and $v_s(s)$ and $v_{ss}(s)$ denote the first and second derivatives of $v(s)$, respectively. The external energy E_{ext} is also minimized based on a summation of the internal energy at the feature of interest, such as the boundary. Given a gray-level image $I(x,y)$, viewed as a function of continuous position variables (x,y), the typical external energy is

$$E_{ext}(x, y) = -|\nabla I(x, y)|^2 \quad (3)$$

where, ∇ is the gradient operator and minimizes the energy function relative to the internal energy using the magnitude in the edge region.

Fig. 1 shows the problems of the conventional active contour model with respect to boundary concavity and initialization. The model has difficulty progressing into a concave region as the elastic and bending energy is depressed. Careful conditions are required for initialization.

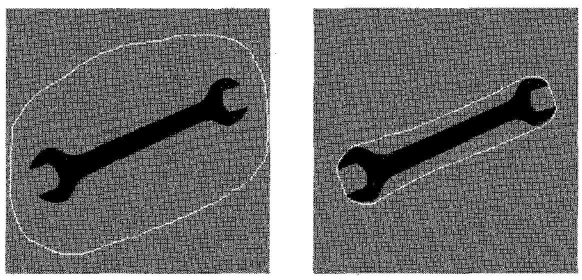

(a) (b)

Fig. 1. (a) Initialization and (b) example of conventional active contour model.

PROPOSED ACTIVE CONTOUR MODEL

In this paper, the new internal energy function controlled by moving the local perpendicular bisector point of each control point on the contour was proposed, and new detection algorithm for multiple objects is implemented in relation to the initial contour by minimizing the energy based on a summation of the internal energy and external energy. Fig. 2 presents a flowchart for detecting an object contour. First, median filtering is implemented for noise removal and edge strengthening, then the initial contour is generated around the region of interest. The contour then moves in the direction to minimize the summation of the internal and external energy. Control points are added or removed from the contour to maintain a regular interval between iterations in relation to the above movement. This iteration process is repeated until the number of control points no longer changes with the convergence of the contour. Multiple objects can then be detected by dividing the contour based on a comparison of a minimum interval for the contour progressing between objects.

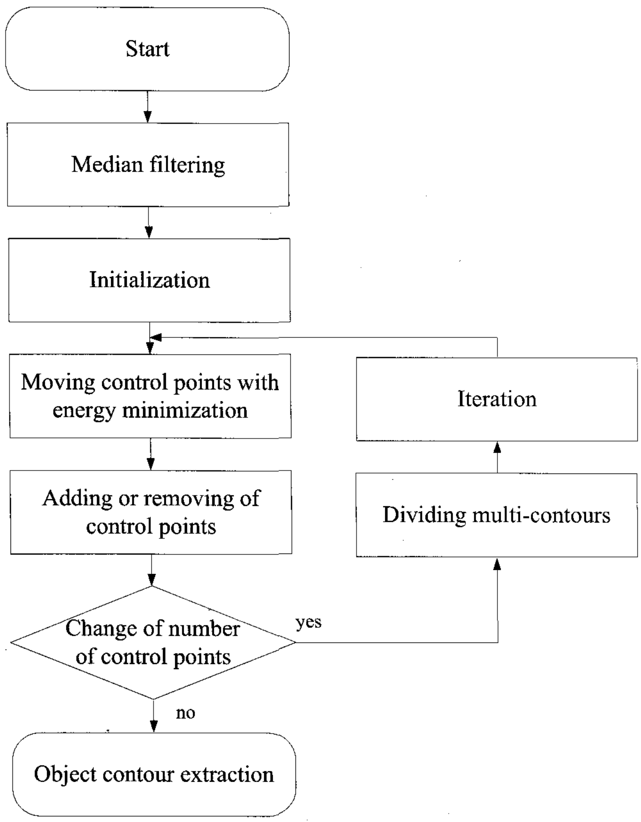

Fig. 2. Flowchart for detection of interest region using active contour model.

Improved Detection of Concave Region

As the preprocessing stage, median filtering removes the noise and strengthens the edges in a medical image. The initial contour is then generated around the object of interest, and initial control points assigned to regularly sample points on the contour. Each assigned control point $v_i(x_i, y_i)$ is moved by controlling the internal energy, as proposed in Eqs. (4) and (5).

$$x_{\text{mid}} = \frac{(x_i + x_{i+1})}{2} \qquad (4)$$
$$y_{\text{mid}} = \frac{(y_i + y_{i+1})}{2}$$

$$\begin{pmatrix} x_i' \\ y_i' \end{pmatrix} = \left(\frac{1}{\cos\theta}\right) \times \begin{pmatrix} \cos\theta & \sin\theta \\ -\sin\theta & \cos\theta \end{pmatrix} \begin{pmatrix} x_{\text{mid}} - x_i \\ y_{\text{mid}} - y_i \end{pmatrix} \qquad (5)$$

where, x_i, y_i is the x, y position of control points, i means i th control point among several control points, $v_{\text{mid}}(x_{\text{mid}}, y_{\text{mid}})$ denotes the mid-point between two control points $v_i(x_i, y_i)$ and $v_{i+1}(x_{i+1}, y_{i+1})$, and $v_i'(x_i', y_i')$ is the point moved to the perpendicular bisector. That is, the contour is moved based on the internal energy controlled using the rotational transform in Eq. (5), and angle θ controls the scale of the internal energy. E_{image} represents the slope of the image in Eq. (6) and is led through a Sobel operator as the first differential operator in Eq. (7).

$$E_{\text{image}} = \gamma \times \nabla I(x_{\text{mid}}, y_{\text{mid}}) \qquad (6)$$

$$\begin{aligned} \nabla I_x(x,y) &= I(x+1,y+1) + 2I(x+1,y) \\ &\quad + I(x+1,y-1) - I(x-1,y+1) \\ &\quad - 2I(x-1,y) - I(x-1,y-1) \\ \nabla I_y(x,y) &= I(x+1,y+1) + 2I(x,y+1) \\ &\quad + I(x-1,y+1) - I(x+1,y-1) \\ &\quad - 2I(x,y-1) - I(x-1,y-1) \end{aligned} \qquad (7)$$

where $I_x(x,y)$ or $I_y(x,y)$ is the slope of x, y direction, respectively, $\nabla I(x_{\text{mid}}, y_{\text{mid}})$ is the sum of two slopes to represent the edge magnitude at $(x_{\text{mid}}, y_{\text{mid}})$

position. γ for control of external energy minimizes the summation of the internal energy as the parameter controlling the energy effect related to the image luminance and background.

Eq. (8) shows that the contour moves toward the direction minimizing the energy function based on the summation $E_{\min}$ of the internal energy E_{int} and external energy E_{ext}.

$$E_{\min} = E_{\text{int}}(x,y) + E_{\text{ext}}(x,y) \tag{8}$$

In Fig 3, the control point on the contour is moved according to the internal energy controlled using the parameter angle θ of the middle points between v_i and v_{i+1}. The movement of the assigned control points on the initial contour then approaches the direction of the region of interest based on iterations in relation to controlling the internal energy. At the edge of the object, the control points are converged using the $E_{\min}$ and continue to progress into a concave region.

In Fig 4, as with the total process in Fig 3, each control point moves along the local perpendicular bisector locations of the control points according to the nth iteration and progresses into a concave region based on an iterative process in relation to controlling the internal energy. In the case of background, the control points on the contour continue to progress, as the internal energy is stronger than the external energy. For an edge with a strong external energy, the control points converged at the edge by energy minimization based on a summation of the internal energy and external energy.

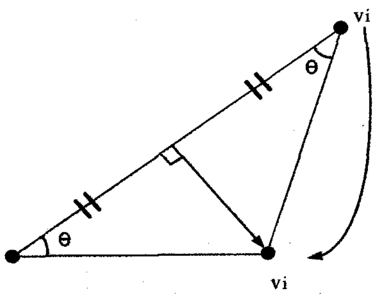

Fig. 3. Movement of control point v_i.

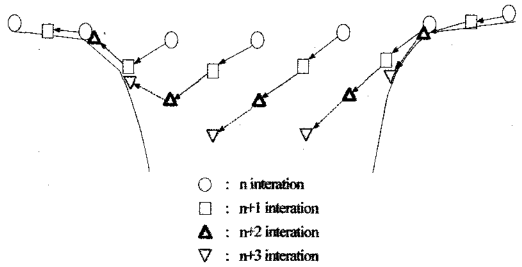

Fig. 4. Movement of control points.

To maintain a regular interval between the control points for each iteration, control point v_{i+1} is removed in the case of a small interval and new control point v_{new} is added in the case of a large interval using Eqs. (9) and (10), respectively

$$\text{if } (distance(v_i, v_{i+1}) \leqq D_{\text{lower}}) \tag{9}$$

$$v_i = v_{i+1}$$

$$else\ \ if\,(distance(v_i, v_{i+1}) > D_{\text{upper}}) \tag{10}$$

$$v_{new}(x,y) = \frac{v_i(x,y) + v_{i+1}(x,y)}{2}$$

where, D_{lower} and D_{upper} denote the reference distance used to reduce two control points to one or add one point to make two points, and $distance(v_i, v_{i+1})$ represents the distance between v_i and v_{i+1}.

Detection of Multiple Objects

Multiple objects can be simultaneously detected by dividing the contours through comparison based on a minimum interval for the contours progressing between the objects. That is, as the interval for the contours progressing between the objects approaches a minimum distance, the contours are divided and converged to each object by an iterative process. However, in the case of a large interval between the objects, the contour cannot be converged to the object, as certain control points on the contours divided by the next iteration may meet again. Thus, to solve this problem, the contour continues to progress after being divided from the control point for the first minimum distance to the next control point, which is larger than a conditional distance.

In the flowchart in Fig. 5, dis_{con} is the condition of the initial minimum distance that divides the contours progressing between the objects, while $dis_{\text{c.p}}$ is the distance between the control points on the contours, and the contour can be divided again by a control point exceeding $\delta \times dis_{\text{con}}$. That is, $Contour_1$ can be divided at the control point of the initial minimum distance and $Contour_2$ is divided at the control point exceeding $\delta \times dis_{\text{con}}$. δ is a parameter for the separation of contours.

In Fig. 6, the first contour, $Contour_1$, is divided at the first minimum distance, where the contour for the upper position and contour for the lower position progressing between the objects approach each other. Then, the second contour, $Contour_2$, is divided again where the distance exceeds the condition as in Fig. 5. The iterative process is finished when the number of control points no longer changes, thereby allowing multiple objects to be simultaneously detected from the initial contour.

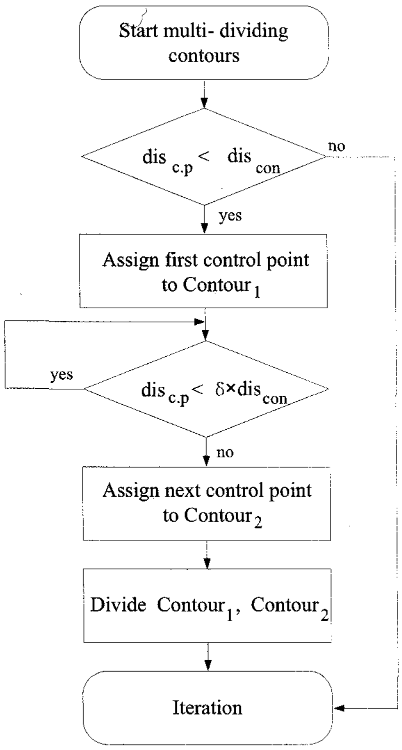

Fig. 5. Flowchart for multi-object detection.

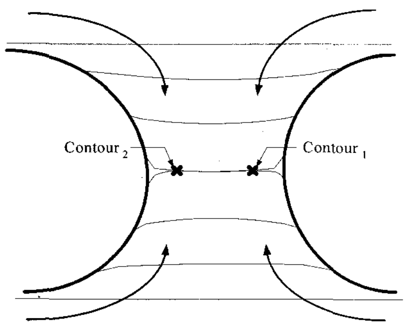

Fig. 6. Movement and separation of contour among objects.

RESULT

Fig. 7(a) shows that the contour converged after ten iterations in a concave region using the proposed method, while Fig. 7(b) shows the improved result from the conventional method in Fig. 1(b). In addition, Fig. 7 (c) shows the multiple objects detection is possible by using proposed method. As such, it was verified that the contour properly converged with the object of interest using the proposed method.

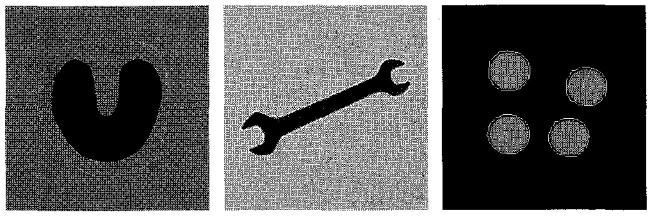

(a) (b) (c)

Fig. 7. (a) Ten iterations and convergence of initial contour and (b) improved spanner image (c) four objects detection.

The validity of the proposed method was confirmed based on a comparison of the square root average error E_{rms} and contour size C_{size} between the conventional method and the proposed method.

$$E_{rms} = \sqrt{\frac{1}{N}\left\{\sum_{i=0}^{N-1}(r(i)-c(i))^2\right\}} \quad (11)$$

E_{rms} denotes the distance error value between the control points $r(i)$ on the reference contour and the control points $c(i)$ on the comparison contour, and N represents the number of control points on the comparison contour.

Fig. 8 shows the reference images used to validate the detection of a concave region and multiple objects, and Fig. 8(b) shows the basic model specifically considered for a pulmonary EBT image.

Fig. 9 shows that the contour was unable to progress into a concave region and did not detect the two objects when using conventional active contour models: initial active contour model, dynamic programming, and greedy algorithm. Conversely, in Fig. 10, the contour naturally progressed into a concave region and the two contours also exactly detected the two objects using the proposed method. In this simulation, contour parameters used are iteration number= 80, α= 0.68, β= 0.051 for all the active contour model, and for the proposed algorithm δ = -0.9. For the GVF parameters are iteration number=125 α= 0.05, β= 0, γ= 0.05, κ= 0.6, and μ= 0.2.

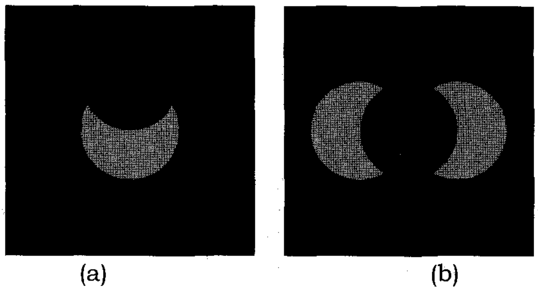

Fig. 8. (a) Reference image I and (b) reference image II for validation.

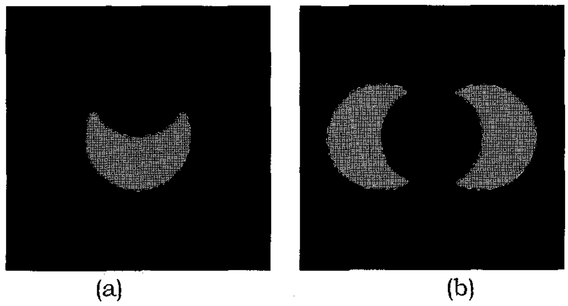

Fig. 10. Examples of the proposed active contour models.

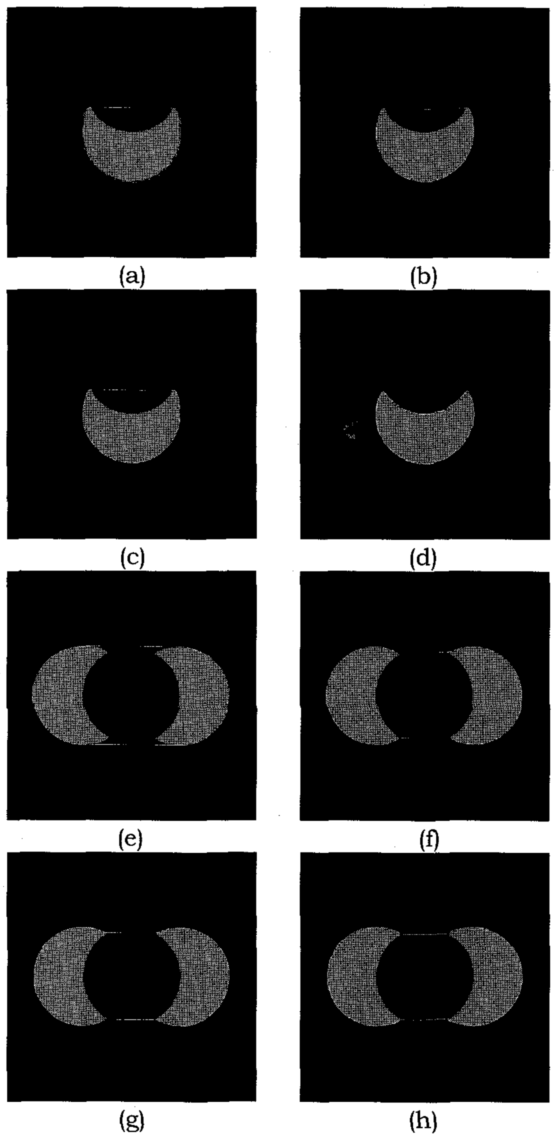

Fig. 9. Examples of the conventional active contour models: (a) and (e) images using initial active contour model, (b) and (f) images using greedy algorithm, (c) and (g) images using dynamic programming (d) and (h) images using GVF.

Table I verifies the improved result using the proposed method through a comparison of the E_{rms} and C_{size} in reference images I and II.

Conventional, Greedy, and Dynamic algorithm have unsatisfying results in Table 1 because of concavity problem and multiple objects. GVF has a good result in Reference I, but in case of Reference II, the results are not satisfying. So, GVF method does not work very well on detection of concave multiple objects like lung region.

Accordingly, the effectiveness of the proposed method was verified based on a comparison with other conventional methods through objective validation and subjective consideration such as the detection of a concave region and multiple objects.

Thereafter, 12-bit quantized images, 512×512 in size, from EBT image equipment (Imatron, Inc.) were used to detect the contour of the pulmonary parenchyma in pulmonary EBT images. Figs. 11 and 12 show the detected right and left pulmonary parenchyma from an initial contour using the proposed solution for concave regions per each slice of tomograpic image, resulting in a 3-dimensional image stack.

Fig. 11. (a) and (b) Examples of pulmonary EBT image using improved active contour model.

Table 1. Algorithm performance comparison

Measure \ Method		Conventional	Greedy	Dynamic	GVF	Proposed
Reference I	E_{rms}	3.380	2.924	3.003	1.112	1.456
	C_{size}	0.723	0.7664	0.7637	0.980	0.938
Reference II	E_{rms}	2.730	2.317	2.410	2.316	1.476
	C_{size}	0.535	0.563	0.564	0.574	0.936

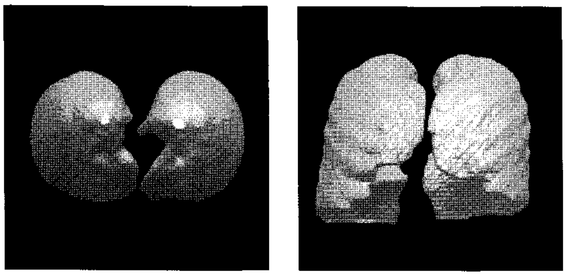

(a) (b)

Fig. 12. 3-dimensional images of pulmonary parenchyma (a) top and (b) frontal views.

CONCLUSION

Conventional active contour models have weak points in relation to concave regions and initialization. Accordingly, this paper proposes a method that allows the contour to progress into a concave region by minimizing the summation of the internal energy controlled based on the movement of a perpendicular bisector by a rotational transform and the external energy generated from the image edge. Using this solution for concave regions, the contours of multiple objects are obtained by dividing the contours based on a comparison with a minimum interval for contours progressing between objects. The contour can be accurately detected by properly controlling parameter θ for the internal energy and parameter γ for the external energy in relation to the features of the object. The proposed method was verified through objective validation and subjective consideration of the detection of concave regions and multiple objects. Consequently, it is expected that the proposed method can be efficiently applied to the early detection of pulmonary disease, and monitoring its progress and healing process through the detection of the pulmonary parenchyma region in medical images.

REFERENCES

[1] C. H. Won, M. N. Kim, J. M. Lee, T. J. Choi, D. S. Kang, *"Diagnosis of Diffuse Lung Disease by quantitative Analysis"*, J. Biomed. Eng. Res., Vol. 20, No. 5, pp. 545-557, 1999.

[2] M. N. Kim, C. H. Won, *"The Contour Extraction of Lung Parenchyma on the EBT Image Acquired with Spirometric Gating"*, J. of the Korean Sensors Society, Vol. 8, No. 2, pp. 154-162, 1999.

[3] N. Ostu. *"A threshold selection method form gray level histogram"*, IEEE Trans. on System, Man and Cybern., Vol. SMC-9, pp. 62-66, 1979.

[4] V. Torre and T. Poggio, *"On edge detection"*, IEEE Trans. on Pattern Analysis and Machine Intelligence, Vol. 8, pp. 147-163, 1986.

[5] C.H. Chu, E.J. Delp, and A.J. Buda, *"Detecting left ventricular endocardial and epicardial boundaries by digital two-dimensional echo-cardiography"*, IEEE Trans. on Med. Imaging, Vol. 7, pp. 81-90, 1988.

[6] M. Kass, A. Witkin, and D. Terzopoulos, *"Snakes: Active contour models"*, Int. j. Computer Vision, Vol. 1, pp. 321-331, 1987.

[7] A.A. Amini, S. Tehrani, and T.E. Weymouth, *"Using dynamic programming for minimizing the energy of active contours in the presence of hard constraints"*, In Proc. Second Int. Conf. on Computer Vision, pp. 95-99, 1988.

[8] D.J. Williams and M. Shah, *"A fast algorithm for active contours and curvature estimation"*, Computer Vision, Graphic, and Image Processing: Image Understanding, Vol. 55, No. 1, pp. 14-26, 1992.

[9] C. Xu and J. L. Prince, *"Snakes, Shapes, and Gradient Vector Flow"*, IEEE Transactions on Image Processing, 7(3), pp. 359-369, March 1998.

[10] C. Xu and J.L. Prince, *"Gradient Vector Flow: A New External Force for Snakes"*, Proc. IEEE Conf. on Comp. Vis. Patt. Recog., Los Alamitos: Comp. Soc. Press, pp. 66-71, June 1997.